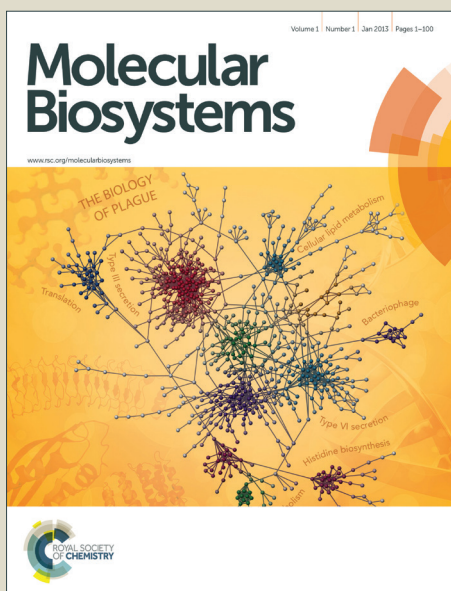


Molecular BioSystems

Accepted Manuscript



This is an *Accepted Manuscript*, which has been through the Royal Society of Chemistry peer review process and has been accepted for publication.

Accepted Manuscripts are published online shortly after acceptance, before technical editing, formatting and proof reading. Using this free service, authors can make their results available to the community, in citable form, before we publish the edited article. We will replace this *Accepted Manuscript* with the edited and formatted *Advance Article* as soon as it is available.

You can find more information about *Accepted Manuscripts* in the [Information for Authors](#).

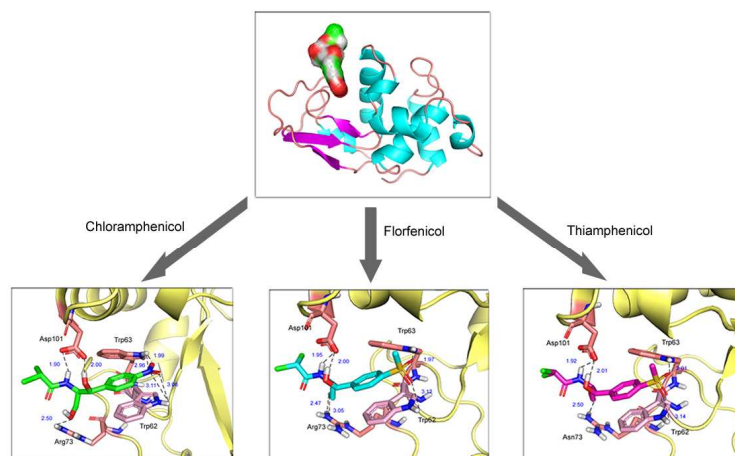
Please note that technical editing may introduce minor changes to the text and/or graphics, which may alter content. The journal's standard [Terms & Conditions](#) and the [Ethical guidelines](#) still apply. In no event shall the Royal Society of Chemistry be held responsible for any errors or omissions in this *Accepted Manuscript* or any consequences arising from the use of any information it contains.



www.rsc.org/molecularbiosystems

Graphic for Table of Contents

The molecular recognition of amphenicols by low-molecular-weight protein may have great impacts on the pharmacokinetics of amphenicols in the human body.



Renal Protein Reactivity and Stability of Antibiotic Amphenicols: Structure and
Affinity

Fei Ding,^{†abc} Wei Peng,^{*†b} Yu-Kui Peng^{*a} and Yu-Ting Jiang^d

^a *College of Food Science & Engineering, Northwest A&F University, Yangling
712100, China*

^b *Department of Chemistry, China Agricultural University, Beijing 100193, China*

^c *Department of Biological Engineering, Massachusetts Institute of Technology,
Cambridge, MA 02139, United States*

^d *Department of Chemistry, University of Ottawa, 10 Marie Curie, Ottawa, ON K1N
6N5, Canada*

[†]These authors contributed equally to this work.

*Corresponding Author

E-mail: pyk2009@nwsuaf.edu.cn (Y.-K. Peng). Phone/fax: +86-29-87092367.

E-mail: jurryw.peng@gmail.com, weipeng@cau.edu.cn (W. Peng). Phone/fax:
+86-10-62734195.

1 **ABSTRACT:** In the present context, the molecular recognition of the oldest active
2 amphenicols by the most popular renal carrier lysozyme was deciphered by using
3 fluorescence, circular dichroism (CD) as well as molecular modeling at the molecular
4 scale. The data of steady state fluorescence showed that the recognition of amphenicol
5 with lysozyme yield fluorescence quenching by a static type, this corroborates
6 time-resolved fluorescence that lysozyme-amphenicol adduct formation has a
7 moderately affinity of 10^4 M^{-1} , and the driving forces were found to be chiefly
8 hydrogen bonds, hydrophobic and π stacking. Far-UV CD spectra confirmed that the
9 spatial structure of lysozyme was slightly changed with a distinct reduction of α -helix
10 in the presence of amphenicol suggesting partial destabilization of the protein.
11 Furthermore, via extrinsic 8-anilino-1-naphthalenesulfonic acid fluorescence spectral
12 properties and molecular modeling, one could see that the amphenicol binding site
13 was situated at the deep crevice on the protein surface, and ligand was also near to
14 several crucial amino acid residues, such as Trp-62 and Trp-63 and Arg-73.
15 Simultaneously, contrastive studies of protein-amphenicols revealed clearly that some
16 substituting groups, e.g. nityl in the molecular structure of ligands may possess
17 vitally important for the recognition activity of amphenicols with lysozyme. Due to
18 amphenicols connection with fatal detrimental effects and lysozyme has been applied
19 as drug carriers for proximal tubular targeting, the discussion emerged herein is
20 thereby necessary for rational antibiotic use, development of safe antibiotic and
21 particularly a better appraisal of the risk associated with the human exposure of toxic
22 agrochemicals.

23

24 **KEYWORDS:** *amphenicols, lysozyme, fluorescence, molecular modeling, structure*

25 *and activity*

26

27

28

29

30

31

32

33

34

35

36

37

38

39

40

41

42

43

44

45 **INTRODUCTION**

46

47 The contamination of food/farm product by chemical contaminants is a globally
48 public health suspense, and is a main reason of trade problems internationally.
49 Contamination could arise by environmental pollution of the air, water and soil, such
50 as the case with toxic metals, polychlorinated biphenyls and dioxins, or especially
51 through the purposeful apply of varied compounds, e.g. pesticides and animal
52 drugs.¹⁻⁴ In general, the use of antibiotics in livestock has been a mooted issue for
53 many years, but antibiotics in livestock farming is necessary to assist avoid the broad
54 and disastrous effects of diseases in herbs. Sometimes antibiotics have been appended
55 to rear to facilitate growth. As Briggs has indicated,⁵ human contact to antibiotics can
56 take place in many different tracks, but food and drinking water are the most
57 significant pathways of exposure for almost any antibiotics including amphenicols
58 (structure shown in Fig. 1). This opinion held by Briggs was subsequently evidenced
59 by certain studies, which endorsed that more than 90% of human exposure befalls
60 mostly through foodstuffs, and those of animal source ordinarily account for nearly
61 80% of the total exposure.⁶ However, pernicious effects are usually far from direct or
62 apparent, owing to most of those antibiotics are seldom present in unduly large
63 concentrations. Luckily, accumulating evidence strongly shows that low residues of
64 the antibiotics may pile up in the fatty tissue, kidney and liver of animals and these
65 are considered to be create several peril to human health.⁷ Furthermore, the use of
66 antibiotics such as amphenicols have plainly been doubted as one of the reasons of the

67 emersion of antibiotic resistant species of bacteria, although the most common root is
68 drecky drug management in the handling of human health.^{8,9} This in reverse sparks
69 off human illness that can not be cured by traditional antibiotics.

70 Fig. 1 here about

71 It was apparent to all that the kidney plays a vital function in the human body's
72 defense against potentially toxic xenobiotics and metabolic waste products through
73 elimination routes. Particularly, secretory vectors in the proximal tubule are
74 outstanding determinants of the treatment of xenobiotics, including many prescription
75 drugs.^{10,11} In accordance with a much recent notion proposed by Dolman et al.,¹² the
76 effectiveness and toxicity of many clinically important drugs and poisonous
77 environmental agents in the body is resolved by their interaction with the renal
78 carriers system. As the proximal tubule is the main site of excretion,
79 low-molecular-weight (LMW) proteins, especially lysozyme is the most famous renal
80 transporter for the intracellular shipment of therapeutic compounds into proximal
81 tubule cells.¹³ In the kidney, the drug-LMW protein complex follows the same route
82 as endogenous LMW protein and ends up in the lysosomes of the proximal tubular
83 cells. Lysozyme is one of the proteins most delved in the drug-LMW protein
84 investigations due to the wealth of data regarding it three-dimensional structure,
85 folding and stability. It is an antibacterial enzyme present in a variety of organisms,
86 which exercises its bacteriostatic role via hydrolyzing the β -1,4 linkage between
87 *N*-acetylmuramic acid (NAM) and *N*-acetyl-glucosamine (NAG) of gigantic polymers
88 (NAM-NAG)_n in the peptidoglycan (murein), leading to lysis of Gram-positive

89 bacterial cell walls.¹⁴ Body fluids, e.g. tears, saliva, urine and human milk comprise
90 2.6, 0.13, trace, and 0.2~0.4 mg mL⁻¹ of lysozyme, respectively. The lysozyme from
91 chicken egg white is structurally highly homologous to lysozyme human, whose
92 diverse variants (Ile-56-Thr and Asp-67-His) from immense amyloid accumulates in
93 the liver and kidneys of the individuals influenced by a hereditary systemic
94 amyloidosis.¹⁵ Therefore, lysozyme is frequently an essential target for toxicity
95 because of its rich vehicle role and focused ability and has been advisedly used as
96 drug transporters for proximal tubular targeting.

97 Currently, binding of a small drug molecule to a LMW protein is requested to alter
98 the receptor's dynamics and conformations and affinities, aiming at governing the
99 protein's functions. Concrete protein-ligand adducts can also be regulated by other
100 small molecules that have similar physicochemical properties, begging for a
101 quantitative estimation of binding specificity at the molecular level.¹⁶ Furthermore,
102 the intrinsic activity of the drug, together with the number of available coupling sites
103 in the carrier macromolecule, determines and thereby also affects the essential amount
104 of carrier protein. Thus both pharmacokinetic and biological parameters need to be
105 taken into account when assessing a LMW protein-drug adduct.¹⁷ For the above
106 reasons, the scope of the present work was to scrutinize the complexation as well as
107 the structure of the complexes formed between the dangerous antibiotic amphenicol
108 and the LMW protein lysozyme, by means of steady state fluorescence, time-resolved
109 fluorescence spectra and extrinsic 8-anilino-1-naphthalenesulfonic acid (ANS) probe.
110 Moreover, the conformation of lysozyme after complexation was monitored by

111 circular dichroism (CD) and, in particular, two other amphenicols, that is
112 thiamphenicol and florfenicol which are all powerful antibacterial compounds and
113 developed in the United States for use exclusively in veterinary medicine, were chose
114 for comparatively analyzing the binding mode between drug and lysozyme based on
115 the computer-aided molecular modeling. Evidently, the study of protein-amphenicols
116 could provide a better comprehension of the biointeraction happening between
117 charged macromolecules and therefore giving perception into processes that occur in
118 several biological systems.

119

120 **EXPERIMENTAL**

121

122 **Materials.** Lysozyme from chicken egg white (L4919, BioUltra, lyophilized
123 powder, \geq 98%), chloramphenicol (C0378, 98%) and
124 8-anilino-1-naphthalenesulfonic acid (A1028, \geq 97%) were purchased from
125 Sigma-Aldrich (St. Louis, MO) and used without further purification, and deionized
126 water was generated by a Milli-Q Ultrapure Water Purification Systems from
127 Millipore (Billerica, MA). Tris (0.2 M)-HCl (0.1 M) buffer of pH=7.4, with an ionic
128 strength 0.1 in the presence of NaCl, except where specified, was used, and the pH
129 was measured with an Orion Star A211 pH Benchtop Meter (Thermo Scientific,
130 Waltham, MA). Dilutions of the lysozyme stock solution (10 μ M) in Tris-HCl buffer
131 were prepared immediately before use, and the concentration of protein was
132 determined by the method of Lowry et al.¹⁸ All other reagents employed were of

133 analytical grade and received from Sigma-Aldrich.

134 **Steady State Fluorescence.** Steady state fluorescence was obtained on a F-7000
135 spectrofluorimeter (Hitachi, Japan) equipped with 1.0 cm quartz cell and a
136 thermostatic cell holder with stirrer. The excitation and emission slits were set at 5.0
137 nm each, intrinsic fluorescence was recorded by exciting the continuously stirred
138 protein solution at 295 nm to selectively excite the tryptophan (Trp) residues, and the
139 fluorescence emission spectra were registered in the wavelength range of 300~450
140 nm at a scanning speed of 240 nm min⁻¹. The reference sample of the Tris-HCl buffer
141 and chloramphenicol did not give any fluorescence signal.

142 **Extrinsic ANS Displacement.** In the first series of experiments, lysozyme
143 concentration was kept fixed at 4.0 μM, and chloramphenicol/ANS concentration was
144 varied from 5.0 to 35 μM, lysozyme fluorescence was gained ($\lambda_{\text{ex}}=295$ nm, $\lambda_{\text{em}}=337$
145 nm). In the second series of experiments, chloramphenicol was added to solutions of
146 lysozyme and ANS held in equimolar concentration (4.0 μM), and the concentration
147 of chloramphenicol was also varied from 5.0 μM to 35 μM, the fluorescence of ANS
148 was recorded ($\lambda_{\text{ex}}=370$ nm, $\lambda_{\text{em}}=465$ nm).

149 **Molecular Modeling.** Molecular modeling of the lysozyme-amphenicols
150 conjugation was conducted on SGI Fuel Workstation. The crystal structure of
151 lysozyme (entry codes 4HP0),¹⁹ determined at a resolution 1.19 Å, was retrieved from
152 the Brookhaven Protein Data Bank. After being imported in the program Sybyl
153 version 7.3, protein structure was carefully inspected for atom and bond type
154 correctness assignment. Hydrogen atoms were computationally added using the Sybyl

155 Biopolymer and Build/Edit menus. To avoid negative acid/acid interactions and
156 repulsive steric clashes, added hydrogen atoms were energy minimized with the
157 Powell algorithm with a convergence gradient of $0.5 \text{ kcal (mol \AA)}^{-1}$ for 1,500 cycles;
158 this procedure does not change positions of heavy atoms, and the potential of the
159 three-dimensional structure of lysozyme was assigned according to the AMBER force
160 field with Kollman all-atom charges. The two-dimensional structures of amphenicols
161 were downloaded from PubChem, and the initial structures of these molecules were
162 generated by Sybyl 7.3. The geometry of amphenicols was subsequently optimized to
163 minimal energy using the Tripos force field with Gasteiger-Hückel charges, the
164 Surfex-Dock program that employs an automatic flexible docking algorithm was
165 applied to calculate the possible conformation of the ligand that binds to the protein,
166 and the program PyMOL (<http://www.pymol.org/>) was used for visualization of the
167 molecular docking results.

168 **Statistical Analysis.** All assays were executed in triplicate, the mean values,
169 standard deviations, and statistical differences were estimated using analysis of
170 variance (ANOVA). The mean values were compared using student's *t*-test, and all
171 statistic data were treated using the OriginPro Software (OriginLab Corporation,
172 Northampton, MA).

173

174 **RESULTS AND DISCUSSION**

175

176 **Reactive Ability.** For the purpose of depicting the conjugation between the ligand

177 and the macromolecule, steady state fluorescence of quenching of Trp residues in
178 lysozyme at pH=7.4 with different amounts of chloramphenicol was shown in Fig. 2.
179 Evidently, lysozyme exhibited a fluorescence emission peak at 337 nm, following an
180 excitation at 295 nm, and the addition of chloramphenicol aroused a gradual reducing
181 of the fluorescence signal. Under the experimental conditions, chloramphenicol
182 behaved no fluorescence emission in the range 300~450 nm which did not affect
183 lysozyme intrinsic Trp fluorescence. These phenomena illustrated clearly there were
184 reactions between protein and chloramphenicol, and chloramphenicol located in the
185 domain where Trp residue situated within or near the fluorophore.²⁰ Similar finding
186 has also been announced by Agudelo et al.²¹ for the binding of chitosan nanoparticles
187 to milk β -lactoglobulin.

188 Fig. 2 here about

189 As noted earlier, binding of ligands to proteins is specially vital as it can influence
190 the distribution and elimination of the ligand as well as the duration and strength of its
191 pharmacological and toxicological action, thus it is necessary to grasp the affinity of
192 chloramphenicol to lysozyme. The inset of Fig. 2 indicates the plot of $\log(F_0 - F)/F$
193 *versus* $\log[Q]$ according to equation (3) (Supporting Information) for the
194 chloramphenicol-lysozyme mixture from fluorescence titration, the calculated
195 association constant fitted from Fig. 2 was $K=2.234 \times 10^4 \text{ M}^{-1}$ ($R=0.9991$) and the
196 value of n is approximately equal to 1. From the point of sight of Kragh-Hansen,²²
197 and combined with the recent publications on the theme of protein-ligand, such as
198 alkanone flavors, α -lactalbumin, quercetin, quercitrin, retinol, retinoic acid, retinal,

199 β -carotene, α -carotene and β -cryptoxanthin,²³⁻²⁷ it is quite obvious that the
200 biointeraction of chloramphenicol with lysozyme belongs to moderate affinity with
201 respect to the other strong protein-ligand complexes with affinities ranging from 10^6
202 to 10^8 M^{-1} . As has been argued, the reabsorptive and secretory duties of the renal
203 tubule are operated by a variety of membrane carriers located in the basolateral and
204 luminal membranes of the tubular epithelium. If a diminish in the binding of a drug to
205 a transporter can yield a growth in the amount of distribution of the drug when the
206 volume of allocation is computed as the ratio of the quantity of drug in the body to the
207 drug concentration in the target organ.²⁸ Thereby we believe that the free
208 concentration of chloramphenicol in the kidney is so large when it enters the human
209 body through food chain. This deduction may possibly be authenticated by some
210 much earlier *in vivo* studies that chloramphenicol is quickly absorbed, inactivated and
211 eliminated, and in patients who have normal renal function about 75 to 90 percent of
212 the oral or parenteral treated drug is disposed in the urine.^{29,30} Moreover, the
213 chloramphenicol residues are cleared not only by glomerular filtration, but by active
214 tubular secretion as well. We should pay more attention to this issue, because
215 lysozyme is one of the most important LMW proteins that have been assayed as renal
216 transporter systems for antibiotics delivery to proximal tubular cells. Meantime, the
217 value of $n \approx 1$, which may explain the existence of just one kind of binding site in
218 protein for chloramphenicol. Basically, intrinsic fluorescence of lysozyme is majorly
219 owing to the Trp-62 residue,³¹ from the value of n , chloramphenicol binding site in
220 lysozyme is most likely near the Trp residue. And, based on the thermodynamic

221 equation: $\Delta G^\circ = -RT \ln K$, we can also compute the Gibbs binding free energy $\Delta G^\circ =$
222 $-24.81 \text{ kJ mol}^{-1}$, which implies that the formation of lysozyme-chloramphenicol
223 adduct was an exothermic reaction.

224 **Reactive Properties.** To explain the nature of fluorescence quenching, the raw
225 data were analyzed according to the well-known Stern-Volmer equation (2), and the
226 corresponding results fitted from Fig. S1 (Supporting Information) was found to be y
227 $= 0.01839x + 0.9803$ ($R = 0.9996$), $K_{SV} = 1.839 \times 10^4 \text{ M}^{-1}$ and $k_q = 9.941 \times 10^{12} \text{ M}^{-1}$
228 s^{-1} . Intuitively, a linear Stern-Volmer plot (Fig. S1) is generally indicative of a single
229 type of fluorophore, all equivalently accessible to quencher. The value of bimolecular
230 quenching constant k_q is about 3 orders of magnitude larger than the maximum value
231 for diffusion-controlled quenching in water ($\sim 10^{10} \text{ M}^{-1} \text{ s}^{-1}$), so it obviously declares
232 that some type of binding interaction happened between lysozyme and
233 chloramphenicol. It is important to recognize that observation of a linear
234 Stern-Volmer plot does not prove that collisional quenching of fluorescence has
235 occurred, where the measurement of fluorescence lifetimes is the most definitive
236 method to distinguish static and dynamic quenching. As can be seen from Table S1,
237 Trp residues are known to signify multiexponential decays, we have not tried to
238 appoint the individual components, on the contrary, the average fluorescence lifetime
239 has been used in order to receive a qualitative analysis. The average fluorescence
240 lifetime of lysozyme decreases from 1.85 ns to 1.66 ns, stating patently that the
241 quenching of lysozyme fluorescence by chloramphenicol is probably static
242 quenching.³²

243 **Circular Dichroism.** As is well known, binding of a ligand to proteins or catalyze
244 typically induces alteration to their three-dimensional structure in most cases, then a
245 realization of structure, in turn, is essential to the discussion of function joins
246 fundamental with the protein-ligand affinity.³³ To analyze the structural changes of
247 lysozyme quantitatively, the raw CD spectra of the protein in the absence and
248 presence of chloramphenicol were shown in Fig. S2, and secondary structure
249 components based on CD data were listed in Table S2. Obviously, the CD curves
250 exhibited two negative peaks in the far-UV CD region at 208 nm and 222 nm,
251 characteristic of a α -helical structure of protein. A reasonable explanation is that the
252 negative peaks between 208 and 209 nm and 222 and 223 nm are both contributed by
253 the $\pi \rightarrow \pi^*$ and $n \rightarrow \pi^*$ transitions of amide groups, and thereby are influenced by the
254 geometries of the polypeptide backbones.³⁴ Table S2 shows that free lysozyme
255 contains 42.1% α -helix, 17.6% β -sheet, 14.4% turn and 25.9% random coil, upon
256 complex with chloramphenicol, diminution of α -helix was observed from 42.1%
257 α -helix free lysozyme to 34.3% complex, while increase in β -sheet, turn and random
258 coil from 17.6%, 14.4% and 25.9% free lysozyme to 19.3%, 17.2% and 29.2%
259 complex. The decline of α -helix with an increase in β -sheet, turn and random coil
260 revealed that chloramphenicol complexes with the amino acid residues of the
261 polypeptide chain, i.e. the biological interactions of amphenicol with LMW protein
262 evoked spatial structural destabilization in lysozyme conformation, which can
263 probably be correlated with its physiological function.^{35,36}

264 **Hydrophobic ANS Probe.** The goal of executing ANS studies was to further

265 confirm the essence of the chloramphenicol recognition by lysozyme. According to
266 the protocol, binding studies were executed in the presence of ANS under identical
267 conditions, and the relative fluorescence (F/F_0) against ligand concentration
268 ([Ligand]) plots is denoted in Fig. S3. Evidently, at a ligand concentration of 45 μM ,
269 both chloramphenicol and ANS had a similar quenching effect on lysozyme
270 fluorescence, i.e. chloramphenicol could quench about 71.57%, and ANS
271 approximately 76.86%. Nevertheless, when chloramphenicol is added to the
272 ANS-lysozyme complex, the fluorescence of ANS-lysozyme missed nearly 21.76%.
273 Stryer^{37,38} has described that interaction of ANS with the solvent exposed
274 hydrophobic clusters of proteins leads to a considerable augment of ANS fluorescence
275 intensity. At present, the fluorescence intensity of ANS-lysozyme disappeared 21.76%
276 upon the addition of chloramphenicol, indicating that chloramphenicol can compete
277 against ANS moderately for its binding site, then the ANS-lysozyme fluorescence
278 would decrease. This corroborates the following results of molecular modeling
279 placing the chloramphenicol at the active site of lysozyme, which constituted by a
280 deep crevice.

281 **Molecular Modeling.** To capture comprehensive insight into the conjugation
282 between lysozyme and antibiotic chloramphenicol, we conduct computational studies
283 and emphasize the important intermolecular interactions between rigid ligand and
284 potential binding clefts on known crystal structure of lysozyme. Based on the
285 high-resolution X-ray diffraction measurement of lysozyme, the active site of the
286 LMW protein consists of a deep crevice, which divides the protein into two domains

287 linked by an α -helix. One domain (residues 40 to 85) comprises almost entirely of
288 β -sheet structure, while the second domain (residues 89 to 99) is more helical.³⁹ The
289 best energy pictures are shown in Fig. 3, it can be perceived that the chloramphenicol
290 fills the groove on the surface of the receptor lysozyme (Fig. 3(A)), thereby the
291 interaction of antibiotic chloramphenicol with lysozyme clearly belongs to the sphere
292 of biochemical reaction on biomacromolecule surface. The nitrogen atom and the
293 oxygen atom of the nitril, the oxygen atom of the hydroxyl group-2, the hydrogen
294 atom of the secondary amine, and the hydrogen atom of the hydroxyl group-1 in
295 chloramphenicol can make seven hydrogen bonds with the hydrogen atom of the
296 secondary amine in Trp-62 and Trp-63, the hydrogen atom of the amino group in
297 Arg-73, and the oxygen atom of the carboxyl group in Asp-101 residues (Fig. 3(B)),
298 the bond lengths are 3.11 Å, 3.06 Å, 2.96 Å, 1.99 Å, 2.50 Å, 1.90 Å and 2.00 Å,
299 respectively. On the basis of surface modification of the active site in lysozyme (Fig.
300 3(C)), we discovered that the preferred conformation of chloramphenicol is located at
301 the hydrophobic patch stably that is composed of Trp-62, Trp-63, Leu-75, Cys-76 and
302 Ile-98 residues, indicating evident hydrophobic interactions worked between
303 chloramphenicol and lysozyme. Furthermore, the plane surface of benzene ring in
304 chloramphenicol is parallel to the plane of indole ring in Trp-62 residue perfectly, and
305 the molecular distance between the heart of the benzene ring and the center of the
306 indole ring is 3.10 Å, which illustrated the existence of tenacious π stacking between
307 antibiotic chloramphenicol and LMW protein. In addition, the association affinity and
308 Gibbs free energy of lysozyme-chloramphenicol adduct are $K=2.344 \times 10^4 \text{ M}^{-1}$ and

309 $\Delta G^\circ = -24.93 \text{ kJ mol}^{-1}$, respectively, the experimental result ($K = 2.234 \times 10^4 \text{ M}^{-1}$
310 and $\Delta G^\circ = -24.81 \text{ kJ mol}^{-1}$) is immensely close to the theoretical value,
311 authenticating the believability of the data on steady state fluorescence illumination.

312 Fig. 3 here about

313 **Exploration of Lysozyme-Thiamphenicol/Florfenicol Adducts.** Thiamphenicol
314 and, more recently, florfenicol, which have molecular structures similar to that of
315 chloramphenicol, appears to reserve the antibacterial properties, decrease strikingly
316 the metabolism by the liver, promote kidney excretion, and eliminate the occurrence
317 of aplastic anemia, although it is possibly more subject to evoke dose-dependent
318 reversible depression of the bone marrow.⁴⁰⁻⁴² These properties make them preferably
319 in certain cases to chloramphenicol. Commonly, thiamphenicol is proposed for the
320 treatment and control of respiratory and intestinal diseases in cattle and poultry. It
321 may also act as a reasonable replacement for other antibiotics that present long
322 depletion times in aquaculture.⁴³ While florfenicol has been permitted for treatment of
323 bovine respiratory disease in the United States, and has also been recently approved in
324 Japan for use by the aquaculture industry to preclude yellowtail disease.⁴⁴ In order to
325 further comprehend the binding mode between chloramphenicol and lysozyme and
326 give some general clues to the amphenicols, thiamphenicol and florfenicol were
327 selected and we have performed preliminarily comparative analyses regarding the
328 recognition properties between the amphenicols and the LMW protein lysozyme by
329 using computer-aided molecular modeling. The best docking energy results are shown
330 in Fig. 4, and the definite noncovalent bonds and bond lengths/distances are collected

331 in Table 1. The binding modes of thiamphenicol (Fig. 4(A)) and florfenicol (Fig. 4(B))
332 are analogous to the chloramphenicol, that is, chloramphenicol and its structurally
333 analogues, thiamphenicol and florfenicol are located within the trench, which is
334 composed by residues 40 to 85 and residues 89 to 99. More specifically,
335 thiamphenicol and florfenicol can yield hydrogen bonds with several central amino
336 acid residues such as Trp-62, Trp-63, Arg-73 and Asp-101, but the intensity of
337 hydrogen bonds is variant due to structural disparities in amphenicols. Further, the
338 same binding location of amphenicols in LMW protein gives thiamphenicol and
339 florfenicol and the indole ring in Trp-62 residue a guaranty to produce π stacking, and
340 the hydrophobic interactions also existed between lysozyme and amphenicols at the
341 same time.

342 Fig. 4 here about

343 Table 1 here about

344 In view of the molecular modeling described above, we could reasonably point
345 out that there is an apparent discrepancy between amphenicols and lysozyme, and the
346 sequence of binding free energy ΔG° in the molecular recognition was computed as
347 follows: chloramphenicol > thiamphenicol > florfenicol, owing to the slight
348 differences of substituting group in the molecular structure of amphenicols. The
349 distinction can be deduced logically from both the noncovalent interactions and the
350 substituent properties, as explained below. In contrast with the methylsulfonyl group
351 in thiamphenicol and florfenicol, nitril was present on benzene ring in
352 chloramphenicol molecule. This event would allow chloramphenicol to yield more

353 strong hydrogen bonds with lysozyme, because the nitrogen atom of the nitril could
354 serve as a receptor for hydrogen bonds, and then noticeably enhances the noncovalent
355 interactions between chloramphenicol and some amino acid residues such as Trp-62
356 and Trp-63. Therefore, the binding affinity of chloramphenicol to lysozyme is far
357 stronger than thiamphenicol and florfenicol. Nevertheless, thiamphenicol and
358 florfenicol have very similar chemical structures but have only different substituent
359 species in the position-2; if the hydroxyl group in the position-2 of thiamphenicol is
360 turned into fluorine atom, it changes to florfenicol. In the eyes of the number and
361 strength of hydrogen bonds, both hydroxyl group and fluorine atom substitution had
362 an important enhancement effects in the formation of hydrogen bonds. However, the
363 hydroxyl group in the position-2 of thiamphenicol can produce hydrogen bond with
364 amino acid residue Arg-73, but the intensity of hydrogen bond was partly less than
365 that of the fluorine atom. Consequently, the most crucial factor for the toxicity of
366 amphenicols to lysozyme is lying in the substituent kind on the benzene ring (Fig.
367 4(C)); in this case, chloramphenicol is the most toxic amphenicols known to human
368 health. According to the above molecular modeling results, it is also particular to note
369 that binding of both chloramphenicol and its analogues to lysozyme could induce
370 change its congenital dynamics evidently. This phenomenon is obvious for grasping
371 protein behavior better, but also has insinuations for the drug industry. Generally,
372 drugs such as antibiotics are designed to rival their target protein, thereby convincing
373 optimization of potential interactions between drug and protein, which makes the
374 binding stronger. If the recognition also alters the dynamic characters of protein, this

375 change should be taken into account, as it influences the entropy of the protein as
376 well.^{45,46} This element is frequently disregarded in drug design process, which may
377 generate serious side effects to human.

378

379 CONCLUSIONS

380

381 On the whole, renal transport systems play a crucial function in the defense
382 against a vast variety of latently injurious chemicals to which we are continually
383 exposed through drugs, environment, food and occupation. And the current story
384 portrays an integrated experimental and computational modeling method of the
385 biointeractions of the extensively food contaminant amphenicols with the most
386 important carrier in the proximal tubule – lysozyme in aqueous solution at
387 physiological pH=7.4. Fluorescence pointed out that the quenching of Trp residues
388 was the formation of the lysozyme-amphenicol complex, which coincides with the
389 time-resolved fluorescence attesting the conclusion that static mechanism does appear
390 to be predominant in this conjugation, and amphenicol binds to lysozyme reversibly
391 through hydrogen bonds, hydrophobic and π stacking with a moderately affinity of
392 10^4 M^{-1} . The data of CD spectra proclaimed that the compactly spatial structure of
393 lysozyme was obviously disturbed after the addition of amphenicol with a decrease of
394 α -helix accompanied by an increase in β -sheet, turn and random coil, which stood for
395 a partial disruption of protein. According to the results of extrinsic ANS displacement,
396 one can ascertain amphenicol was located at the crevice on the surface of the protein,

397 this matches the molecular modeling placing amphenicol at the hydrophobic region,
398 where Trp-62, Trp-63, Leu-75, Cys-76 and Ile-98 residues on the lysozyme and the
399 Trp-62 and Trp-63 residues are all near to ligand. Through comparative analyses of
400 the molecular recognition of chloramphenicol and its structurally analogues, that is
401 thiamphenicol and florfenicol with lysozyme, we may reasonably understand that the
402 reactivity between lysozyme and chloramphenicol was much higher than that of
403 thiamphenicol and florfenicol. And, several key substituents, such as nitril and
404 methylsulfonyl group on the benzene ring in amphenicols may probably have a great
405 influence on the toxicological action to human health.

ASSOCIATED CONTENT

Supporting Information

Detailed experimental procedures for time-resolved fluorescence and circular dichroism of lysozyme and lysozyme-amphenicol, calculation of reactive ability, Stern-Volmer plot, the plot of extrinsic ANS displacement and the abbreviations used in this manuscript.

AUTHOR INFORMATION

Corresponding Author

*E-mail: pyk2009@nwsuaf.edu.cn. Phone/fax: +86-29-87092367.

*E-mail: jurryw.peng@gmail.com, weipeng@cau.edu.cn. Phone/fax:
+86-10-62734195.

Author Contributions

†These authors contributed equally to this work.

NOTES

The authors declare no competing financial interest.

ACKNOWLEDGEMENTS

We are deeply indebted to Professor Ulrich Kragh-Hansen of Department of Medical Biochemistry, University of Aarhus, for the valuable gift of his doctoral dissertation.

We are particularly grateful to Publishing Editor – Mr. Thadcha Retneswaran of Molecular BioSystems, Royal Society of Chemistry, for his kindly assistance during the manuscript processing. Thanks also go to the reviewers of this manuscript for their priceless and constructive suggestions.

REFERENCES

1. K. Kümmerer, *Annu. Rev. Environ. Resour.*, 2010, **35**, 57-75.
2. J. N. Seiber and L. A. Kleinschmidt, *J. Agric. Food Chem.*, 2011, **59**, 7536-7543.

3. J. N. Seiber and L. Kleinschmidt, *J. Agric. Food Chem.*, 2012, **60**, 6644-6647.
4. K. Armbrust, M. Burns, A. N. Crossan, D. A. Fischhoff, L. E. Hammond, J. J. Johnston, I. Kennedy, M. T. Rose, J. N. Seiber and K. Solomon, *J. Agric. Food Chem.*, 2013, **61**, 4676-4691.
5. D. Briggs, *Br. Med. Bull.*, 2003, **68**, 1-24.
6. http://foodweb.ut.ee/s2/111_94_45_Summary_of_the_selected_contaminants.pdf
7. H. Tajik, H. Malekinejad, S. M. Razavi-Rouhani, M. R. Pajouhi, R. Mahmoudi and A. Haghazari, *Food Chem. Toxicol.*, 2010, **48**, 2464-2468.
8. E. K. Silbergeld, J. Graham and L. B. Price, *Annu. Rev. Public Health*, 2008, **29**, 151-169.
9. B. Berendsen, M. Pikkemaat, P. Römken, R. Wegh, M. van Sisseren, L. Stolker and M. Nielen, *J. Agric. Food Chem.*, 2013, **61**, 4004-4010.
10. R. A. Phillips, *Annu. Rev. Physiol.*, 1949, **11**, 493-526.
11. K. M. Morrissey, S. L. Stocker, M. B. Wittwer, L. Xu and K. M. Giacomini, *Annu. Rev. Pharmacol. Toxicol.*, 2013, **53**, 503-529.
12. M. E. M. Dolman, S. Harmsen, G. Storm, W. E. Hennink and R. J. Kok, *Adv. Drug Deliv. Rev.*, 2010, **62**, 1344-1357.
13. C. Cojocel and K. Baumann, *Renal Physiol.*, 1983, **6**, 258-265.
14. E. A. Johnson and A. E. Larson, in *Antimicrobials in Food*, ed. P. M. Davidson, J. N. Sofos and A. L. Branen, CRC Press, Taylor & Francis Group, Boca Raton, FL, 3rd edn., 2005, pp. 361-387.
15. C. C. F. Blake and I. D. A. Swan, *Nat. New Biol.*, 1971, **232**, 12-15.

16. S. A. Pless and C. A. Ahern, *Annu. Rev. Pharmacol. Toxicol.*, 2013, **53**, 211-229.
17. G. M. Whitesides and V. M. Krishnamurthy, *Q. Rev. Biophys.*, 2005, **38**, 385-395.
18. O. H. Lowry, N. J. Rosebrough, A. L. Farr and R. J. Randall, *J. Biol. Chem.*, 1951, **193**, 265-275.
19. M. Ogata, N. Umemoto, T. Ohnuma, T. Numata, A. Suzuki, T. Usui and T. Fukamizo, *J. Biol. Chem.*, 2013, **288**, 6072-6082.
20. I. Hasni, P. Bourassa and H.-A. Tajmir-Riahi, *J. Phys. Chem. B*, 2011, **115**, 6683-6690.
21. D. Agudelo, S. Nafisi and H.-A. Tajmir-Riahi, *J. Phys. Chem. B*, 2013, **117**, 6403-6409.
22. U. Kragh-Hansen, *Dan. Med. Bull.*, 1990, **37**, 57-84.
23. T. E. O'Neill and J. E. Kinsella, *J. Agric. Food Chem.*, 1987, **35**, 770-774.
24. M. Nigen, V. Le Tilly, T. Croguennec, D. Drouin-Kucma and S. Bouhallab, *Biochem. Biophys. Acta – Proteins Proteomics*, 2009, **1794**, 709-715.
25. M. Sahihi, Z. Heidari-Koholi and A.-K. Bordbar, *J. Macromol. Sci., Part B: Phys.*, 2012, **51**, 2311-2323.
26. A. Belatik, C. D. Kanakis, S. Hotchandani, P. A. Tarantilis, M. G. Polissiou and H. A. Tajmir-Riahi, *J. Biomol. Struct. Dyn.*, 2012, **30**, 437-447.
27. A. Mensi, Y. Choiset, H. Rabesona, T. Haertlé, P. Borel and J.-M. Chobert, *J. Agric. Food Chem.*, 2013, **61**, 4114-4119.
28. M. Rowland, C. Peck and G. Tucker, *Annu. Rev. Pharmacol. Toxicol.*, 2011, **51**, 45-73.

29. R. T. Williams, *Annu. Rev. Biochem.*, 1951, **20**, 441-464.
30. C. M. Kunin, A. J. Glazko and M. Finland, *J. Clin. Invest.*, 1959, **38**, 1498-1508.
31. S. Balme, R. Guégan, J.-M. Janot, M. Jaber, M. Lepoitevin, P. Dejardin, X. Bourrat and M. Motelica-Heino, *Soft Matter*, 2013, **9**, 3188-3196.
32. M. Banerjee, A. Chakrabarti and S. Basu, *J. Phys. Chem. B*, 2012, **116**, 6150-6157.
33. I. Bahar, T. R. Lezon, L.-W. Yang and E. Eyal, *Annu. Rev. Biophys.*, 2010, **39**, 23-42.
34. S. M. Kelly and N. C. Price, *Curr. Protoc. Protein Sci.*, 2006, **46**, 20.10.1-20.10.18.
35. C. D. Kanakis, P. A. Tarantilis, M. G. Polissiou and H. A. Tajmir-Riahi, *J. Biomol. Struct. Dyn.*, 2013, **31**, 1455-1466.
36. F. P. Ziyarat, A. Asoodeh, Z. S. Barfeh, M. Pirouzi and J. Chamani, *J. Biomol. Struct. Dyn.*, 2014, **32**, 613-629.
37. L. Stryer, *J. Mol. Biol.*, 1965, **13**, 482-495.
38. L. Stryer, *J. Biol. Chem.*, 2012, **287**, 15164-15173.
39. S. J. Ford, A. Cooper, L. Hecht, G. Wilson and L. D. Barron, *J. Chem. Soc., Faraday Trans.*, 1995, **91**, 2087-2093.
40. M. Atef, A. Y. I. El-Gendi, A. M. Amer and A. M. A. El-Aty, *Food Chem. Toxicol.*, 2010, **48**, 3340-3344.
41. Y. Berkov-Zrihen, K. D. Green, K. J. Labby, M. Feldman, S. Garneau-Tsodikova and M. Fridman, *J. Med. Chem.*, 2013, **56**, 5613-5625.

42. M. Kołodziejska, J. Maszkowska, A. Białk-Bielińska, S. Steudte, J. Kumirska, P. Stepnowski and S. Stolte, *Chemosphere*, 2013, **92**, 1253-1259.
43. A. Azzouz, B. Jurado-Sánchez, B. Souhail and E. Ballesteros, *J. Agric. Food Chem.*, 2011, **59**, 5125-5132.
44. A. Anadón, M. A. Martínez, M. Martínez, A. Ríos, V. Caballero, I. Ares and M. R. Martínez-Larrañaga, *J. Agric. Food Chem.*, 2008, **56**, 11049-11056.
45. C. F. Wong and J. A. McCammon, *Annu. Rev. Pharmacol. Toxicol.*, 2003, **43**, 31-45.
46. L. Skjærven, L. Codutti, A. Angelini, M. Grimaldi, D. Latek, P. Monecke, M. K. Dreyer and T. Carlomagno, *J. Am. Chem. Soc.*, 2013, **135**, 5819-5827.

Table 1

Noncovalent bonds analyses from the results of molecular modeling for lysozyme with amphenicols

Amphenicols	Noncovalent bonds	Ligands	Lysozyme	Distance (Å)
Chloramphenicol	Hydrogen bonds	--NO_2	Trp-62: --NH	3.11
		--NO_2	Trp-62: --NH	3.06
		--NO_2	Trp-63: --NH	2.96
		--NO_2	Trp-63: --NH	1.99
		OH-2	Arg-73: --NH_2	2.50
		NH-3	Asp-101: --COO	1.90
		OH-1	Asp-101: --COO	2.00
	π stacking	benzene ring (center)	Trp-62: indole ring (center)	3.10
Thiamphenicol	Hydrogen bonds	$\text{--SO}_2\text{CH}_3$: O-6	Trp-62: --NH	3.14
		$\text{--SO}_2\text{CH}_3$: O-5	Trp-63: --NH	2.01
		OH-2	Arg-73: --NH_2	2.50
		NH-3	Asp-101: --COO	1.92
		OH-1	Asp-101: --COO	2.01
	π stacking	benzene ring (center)	Trp-62: indole ring (center)	3.10
Florfenicol	Hydrogen bonds	$\text{--SO}_2\text{CH}_3$: O-6	Trp-62: --NH	3.12
		$\text{--SO}_2\text{CH}_3$: O-5	Trp-63: --NH	1.97
		F-2	Arg-73: --NH_2	2.47
		F-2	Arg-73: --NH_2	3.05
		NH-3	Asp-101: --COO	1.95
		OH-1	Asp-101: --COO	2.00
	π stacking	benzene ring (center)	Trp-62: indole ring (center)	3.10

Figure Captions

Fig. 1. Molecular structures of chloramphenicol (A), thiamphenicol (B), and florfenicol (C).

Fig. 2. Fluorescence emission spectra of 4.0 μM lysozyme at $\lambda_{\text{ex}}=295$ nm showing the quenching effect of increasing concentrations of chloramphenicol (a→h): 0, 5.0, 10, 15, 20, 25, 30 and 35 μM , (x) 35 μM chloramphenicol only. Spectra were recorded at $\text{pH}=7.4$ and $T=298$ K. The inset corresponds to reactivity plot describing lysozyme Trp quenching caused by chloramphenicol biointeraction. $y=1.02x+4.349$, $R=0.9991$, based on equation (3). The λ_{em} maximum occurred at 337 nm and all data were corrected for quencher fluorescence. Each point was the mean of three independent observations \pm S.D. ranging 0.31% – 3.77%.

Fig. 3. Molecular modeling of chloramphenicol docked to lysozyme (panel (A)), the colorized carbon skeleton model displays chloramphenicol, colored as per the atoms and possesses opaque surface of electron spin density. The key amino acid residues around chloramphenicol (green stick) have been implied in stick model, warm pink model exhibits hydrogen bonds (panel (B)) between Trp-62, Trp-63, Arg-73, Asp-101 residues and chloramphenicol; panel (C) illustrates hydrophobic interactions between Trp-62, Trp-63, Leu-75, Cys-76, Ile-98 residues and chloramphenicol (ball-and-stick

model); light pink model (panel (B)) expresses π stacking between Trp-62 residue and chloramphenicol. (For interpretation of the references to color in this figure legend, the reader is referred to the web version of the article.)

Fig. 4. Molecular modeling of thiamphenicol (panel (A)) and florfenicol (panel (B)) docked to lysozyme. The critical amino acid residues around thiamphenicol (magenta stick) and florfenicol (cyan stick) have been manifested in stick model, warm pink stick model presents hydrogen bonds between Trp-62, Trp-63, Arg-73, Asp-101 residues and thiamphenicol and florfenicol, respectively; light pink stick model explains π stacking between Trp-62 residue and thiamphenicol and florfenicol, respectively; panel (C) interprets the superimposable conformations of chloramphenicol, thiamphenicol and florfenicol binding to lysozyme. (For interpretation of the references to color in this figure legend, the reader is referred to the web version of the article.)

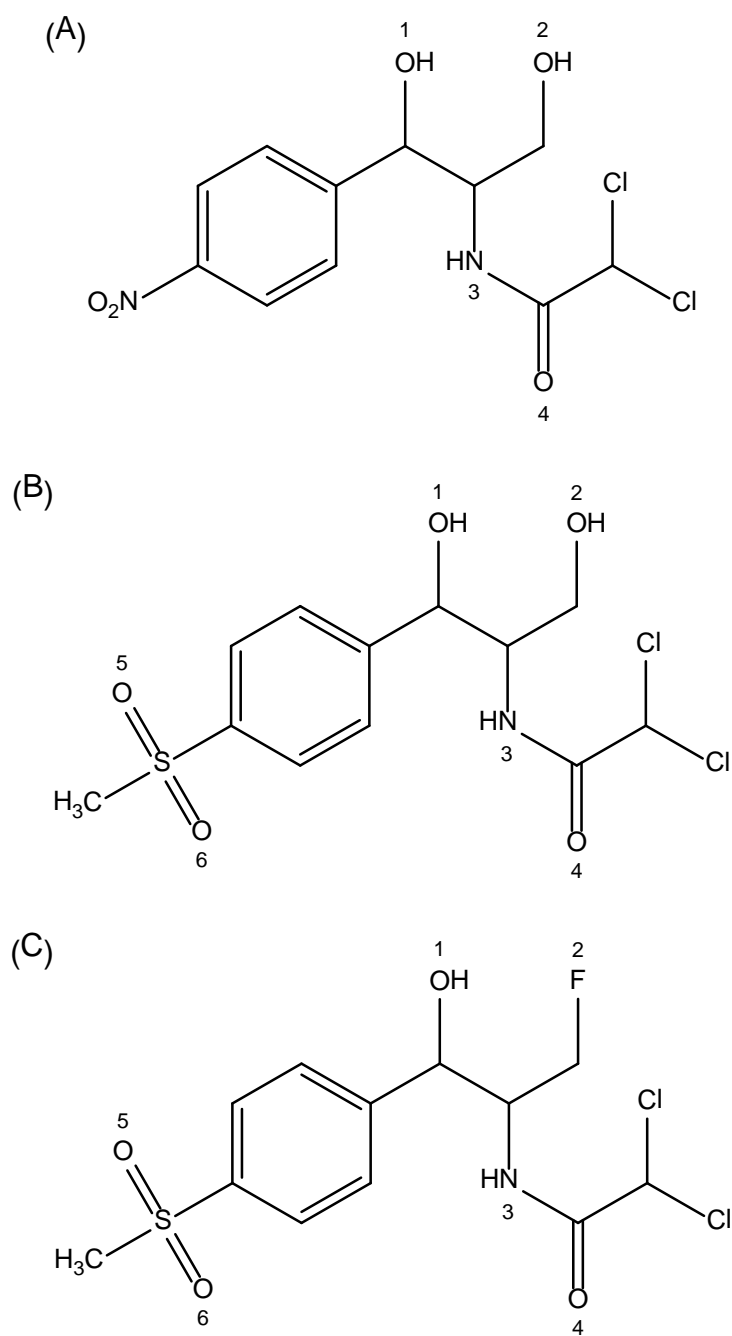


Fig. 1

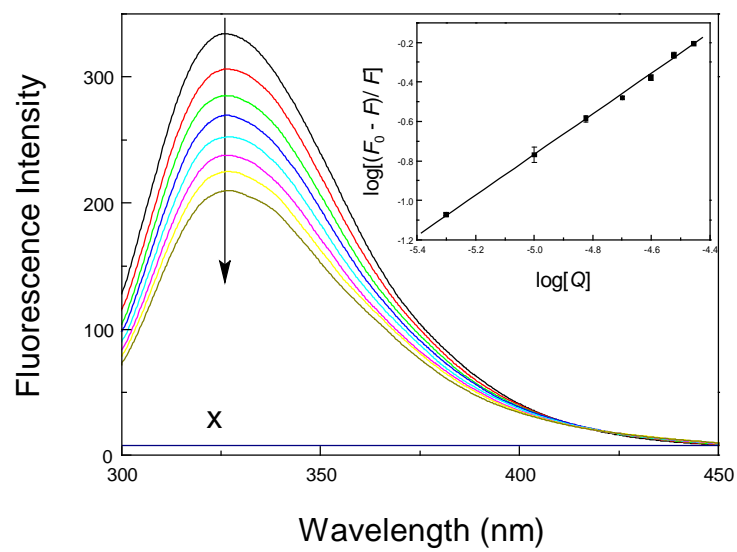


Fig. 2

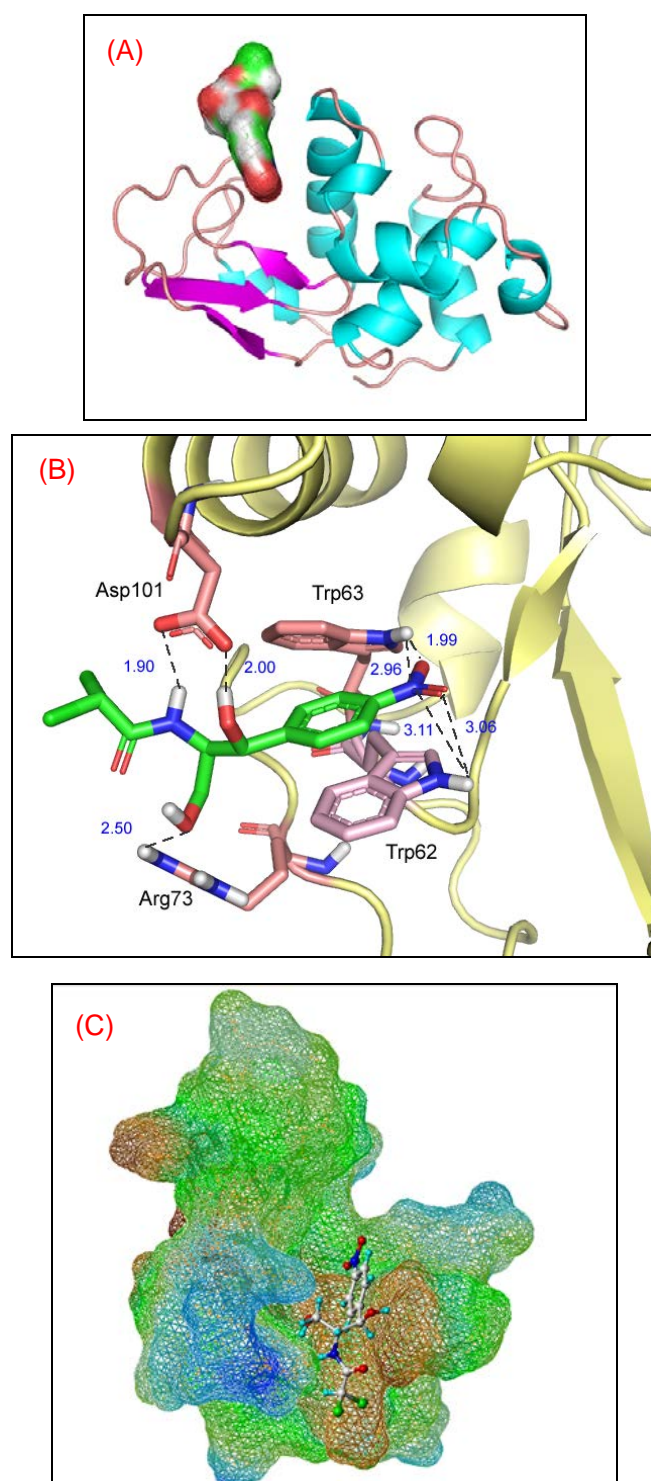


Fig. 3

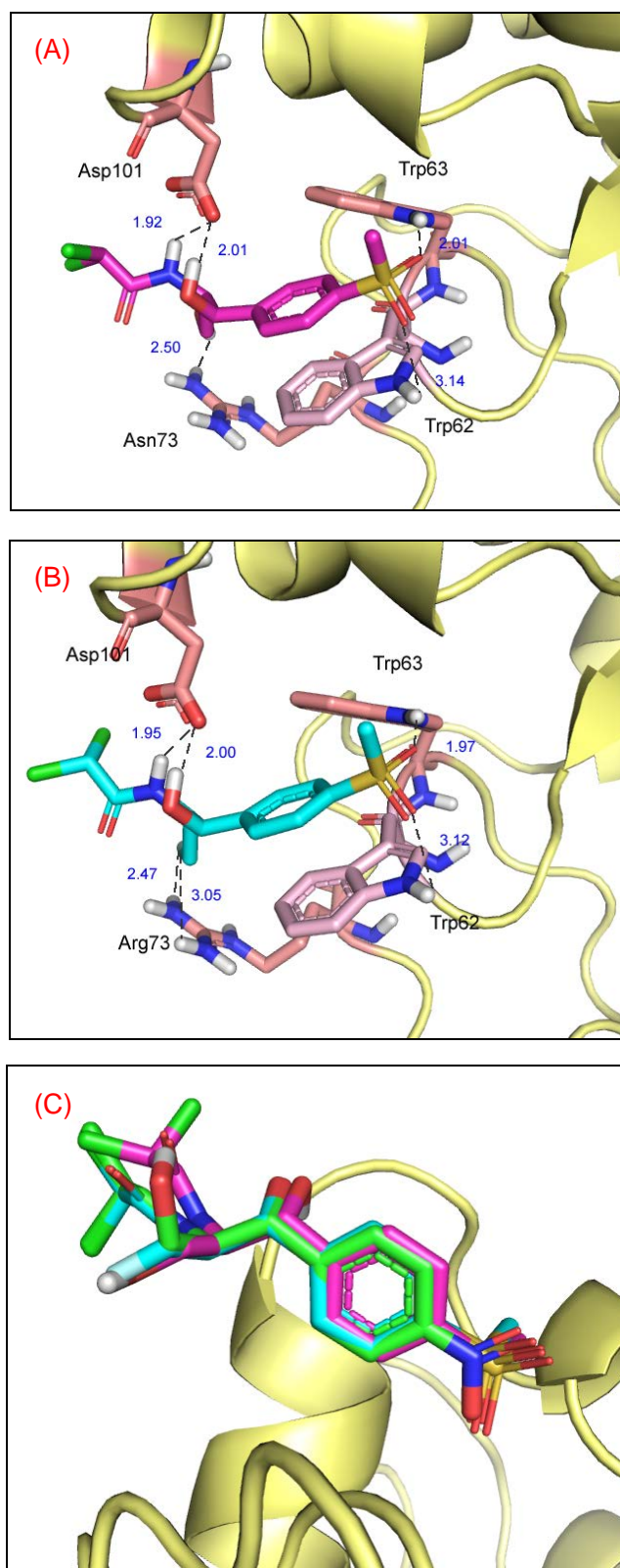


Fig. 4